VIBRATION AND DAMPING OF THIN-WALLED CYLINDERS

Thesis by

George A. Watts

In Partial Fulfillment of the Requirements

For the Degree of

Aeronautical Engineer

California Institute of Technology

Pasadena, California

1962

ABSTRACT

The frequencies of normal modes of free vibration of three cylinders of different thickness were found experimentally. For some of the modes damping was also found. The modes excited were of a single axial half wave and multiple circumferential waves.

The shells were geometrically similar except for thickness and were made by electroplating copper on accurately machined wax mandrels. Melting the wax produced shells of very uniform thickness without seams.

The modes and frequencies agreed to within 10% of the theoretical values for cylinders with fixed ends, except at small numbers of waves where they agreed more closely with the theoretical values for freely supported ends. The damping factors tended toward a small constant value with increasing numbers of waves above the mode with fundamental frequency, but increased rapidly as the numbers of waves decreased below the fundamental.

ACKNOWLEDGMENTS

The author is indebted to the National Aeronautics and Space Administration, Manned Spacecraft Center, for providing the Graduate Study Leave and tuition under which this study has been conducted.

He is also grateful to the United States Air Force Office of Scientific Research for providing the models and most of the equipment.

The author would especially like to thank Professor Y. C. Fung of the California Institute for suggesting the topic of this thesis and for guidance throughout the work.

The many helpful suggestions made by Dr. R. O. Stearman and the assistance with the electronics equipment rendered by Mr. M. E. Jesse also of the California Institute is gratefully acknowledged.

LIST OF SYMBOLS

f	Frequency, c.p.s.
Δf	Increment in frequency between .707 amplitude points, c.p.s.
$N_{\frac{1}{2}}$	Number of cycles to half amplitude
δ	Deflection, inches
δ_o	Initial deflection, inches
t	Time
m	Number of axial half waves
n	Number of circumferential waves
h	Shell thickness, inches
τ	Damping factor
g	Structural damping parameter
Δp	Shell internal gauge pressure, p.s.i.

TABLE OF CONTENTS

I. INTRODUCTION

Thin-walled shells, sometimes pressure stabilized, are used as structural elements in missiles, space vehicles and other applications where minimum weight is important. These structures are often exposed to airflow and turbulence shed by forebodies. To enable the response to fluctuating pressures to be estimated or the aeroelastic stability to be evaluated it is necessary to understand the free motions of the structure and the nature of the damping forces tending to dissipate these motions.

Two theories (1) and (2) have been advanced to predict the natural frequencies and associated modal patterns of cylindrical shells but no significant progress has been made in predicting the decay of the vibration amplitude.

The present experimental investigation was undertaken in an attempt to test the validity of the modal theories for very thin walled shells and to provide vibration decay data.

To this end the natural frequencies associated with modes of a single axial half wave and multiple circumferential waves were found experimentally on three cylindrical

seamless copper shells of 16 inches diameter, 15⅛ inches length, and .020, .0060, and .0032 inches wall thickness. Damping factors were also found for many of these modes by observing the numbers of cycles required for the free vibrations to decay to half amplitude.

Use was made of a model designed for wind tunnel shell flutter experiments. Consequently the shell boundary fixity was dictated by sealing and strength requirements rather than by an attempt to achieve either fixed or freely supported ends.

The work was conducted at the Guggenheim Aeronautical Laboratory of the California Institute of Technology.

II. EQUIPMENT AND PROCEDURE

A. Shells and Support Fixture

The shells were electroplated integrally to heavy copper rings at each end. The ring at the forward end was attached to the heavy aluminum support fixture by machine screws which pulled it into firm contact with a sealing "O" ring in a groove in the support rig as shown in Figure 1. The rear copper ring was attached to a flexible brass diaphragm by means of screws and a rubber gasket and this, in turn, was rigidly attached to the support fixture.

B. Vibration Sensor

The vibration sensor was mounted on a drum free to rotate under the shell through an angular range of 180°. The sensor was also free to traverse fore and aft on the drum from 15% to 67% of the shell length by virtue of a screw jack assembly (see Figures 1 and 2).

The drum was rotated by a small electric motor at an angular velocity of approximately 2/3 of a degree per second or a surface velocity of approximately 1/10 of an inch per second. The fore and aft sensor velocity was somewhat lower. From plots of vibration amplitude vs.

angular and axial positions the mode shapes were determined.

The vibration sensor consisted of a small coil wound around a powdered iron core, the inductance of which varied according to the distance between the coil and the copper shell. Thus the amplified voltage drop across the coil, when energized by a 1.00 kilocycle carrier, provided a measure of the displacement.

In the amplifying electronic circuit the carrier frequency was filtered out leaving only a voltage proportional to the instantaneous displacement. Then this filtered signal was split into A.C. and D.C. components; the A.C. representing the motion of the surface and the D.C., the static position of the surface. All modal analyses were performed using the A.C. portion of the signal. The only effect of static displacement of the surface, such as installation eccentricity and manufacturing tolerance, then was to change the slope of the response curve and, therefore, change the sensitivity of the sensor. Static displacements of this type produced a sensitivity change of approximately 20% over a complete 180° traverse.

C. Analysis Equipment

The wave form of the shell vibration and the time decay of oscillations were studied on a cathode ray oscilloscope.

The root mean square voltage, proportional to the vibration amplitude, was displayed on a vacuum tube voltmeter and the mean square output of the voltmeter was plotted versus either angular or axial position by means of an automatic plotting machine.

A precise measure of the exciting frequency was supplied by an "events per unit time" timer. The unit of time was 10 seconds so that the frequencies were accurate to 1/10 cycles per second.

D. Shell Excitation

Two means of exciting the shell were employed; they were a conventional 30 watt, 8 ohm, loudspeaker with an output between 60 and 6,000 cycles per second and an electrodynamic shaker. The electrodynamic shaker induced an oscillating rotary eddy current locally in the plane of the shell by means of a coil with a powdered iron core and also set up a strong stationary magnetic field from a heavy

permanent magnet mounted in tandem with the coil. The eddy currents, rotating alternately clockwise and counterclockwise, in the presence of the steady magnetic field produced forces normal to the sheet alternately inward and outward. Figure 4 shows schematically the geometric relationship between the eddy currents, magnetic fields and force vector applied to the shell. For a detailed exposition of the shaker design problem, see reference 3.

The main advantage of the electrodynamic shaker is that a sinusoidal force fairly free from sub and superharmonic components can be generated without having to attach any magnetic masses to the test specimen. The method is ideally suited to non-magnetic highly conductive materials such as copper and aluminum.

The shaker was mounted on an external traversing frame so that it could be rotated about the shell to any desired position. In practice, however, it was kept to within 20 degrees of the center of the side opposite the traversing sensor to avoid electrical interference. It could also be traversed axially.

Both the shaker and the speaker were energized by the amplified output from a variable frequency oscillator.

The voltage to the exciter was monitored by a small vacuum tube voltmeter.

E. Measurement of Vibration Decay

The shell was driven to steady state resonant vibration for the desired mode by either the loud speaker or the electrodynamic shaker. Then the exciting force was abruptly stopped by shorting the oscillator output to the amplifier with one throw of a double throw microswitch. The other throw discharged a condenser into the external SYNC. input to the oscilloscope which produced a single slow sweep across the screen and displayed the exponential decay of the vibration, which was photographed.

F. Experimental Procedure

Resonant frequencies were found by mounting the shaker at approximately half way along the shell on the side opposite the sensor. Then with the sensor arbitrarily positioned and the shaker or speaker at about three quarters of its maximum output the frequency was increased from well below the theoretical lowest frequency until a response above the electronic noise level was noted on the

voltmeter. The frequency was carefully adjusted to tune the sensor output to a peak. Then the sensor was rotated to an antinodal position by maximizing the voltmeter signal and the frequency vernier tuned to an accuracy better than 1/10 cycle per second.

At this position a photograph of the vibration decay was made, from which the number of cycles to half amplitude could be obtained and the damping factor determined.

After this, axial and circumferential traverses were made and the mean square voltage (proportional to mean square vibration amplitude) plotted to disclose the mode shape; (that is disclose the number of axial half waves "m" and circumferential waves "n"). During traversing the wave form of the oscillation was monitored on the oscilloscope and the frequency was continually counted on the "EPUT" timer.

After several modes had been found in this manner it was possible to plot the frequency vs. numbers of circumferential waves and by interpolation and extrapolation get approximate values for the modes missed. A trial and error search in the indicated regions usually disclosed the missing modes.

To obtain a check on the damping factors by another method, the vibration amplitude was plotted as a function of frequency near resonance and the width of the curve at .707 of the peak amplitude found. From these values the damping factor was calculated.

In some tests the shell was pressurized and the dependence of resonant frequency on pressurization determined (see Figure 15).

III. RESULTS AND DISCUSSION

A. Resonant Frequencies

Resonant frequencies for m = 1 modes are shown versus n for shells of thickness h = .020, .0060, and .0032 inches in Figures 5, 6, and 7. For comparison the theoretical values of the resonant frequencies by the method of Arnold and Warburton (1) for ends of the shell freely supported and fixed are also shown.

It should be noted that at high values of "n", where theoretically the effect of end fixity becomes unimportant, the experimental values agree quite well with theory.

At values of n near the minimum frequency, where the effect of end fixity is quite important, the curves for shells of thickness h = .020 and .0060 inches lie between the values for fixed and freely supported end fixity; but the .0060 inch shell frequencies approach the fixed ended frequencies. The h = .0032 shell, however, has frequencies considerably higher than theoretically predicted for fully fixed ends. This last result suggested perhaps that some mechanism other than end fixity was at work on the thinner shells to raise the frequency.

Figure 8 shows the experimental data alone. It should be noted that an extrapolation to lower values of n (for the h = .0032 shell) yielded frequencies that rapidly approached the experimental values of frequency for the h = .020 shell. This confirmed the theoretical fact, illustrated in Figure 9 for fixed ended modes, that for low n numbers the natural frequency is independent of thickness for identical end fixity.

The other conclusion to be drawn from this observation is that the effective end fixity of the h = .020 and h = .0032 shells was approximately the same. For if there had been a large difference in the end fixity the frequencies would have been much different at low values of n.

B. Damping

The oscillation decay data is presented in terms of a damping factor τ ; defined as:

$$\tau = \frac{f \log 2}{N_{\frac{1}{2}}}$$

Physically τ corresponds to the exponential decay

factor found in the free vibration of a viscously damped single degree of freedom system:

$$\delta = \delta_0 e^{-\tau t} \cos 2\pi f t$$

and appears to be a reasonable parameter to use in view of the exponential form of the damping actually found (see Figure 14(b); n = 9).

Another term "g" often found in the literature to describe structural damping is related to τ, at least for steady state vibration, as follows:

$$g = \frac{\tau}{\pi f}$$

The experimental values of τ for the shell of wall thickness .0032 inches is shown plotted versus wave number and frequency in Figures 10 and 11. It should be noted that at large values of "n" the decay factor tended to become constant at a value of approximately 1.25. While at small wave numbers below the fundamental mode the factor grew rapidly to a value nearly three times as great at n = 8.

For the shell of wall thickness .020 inches, Figures 12 and 13, at the maximum number of waves excited the decay factor was approximately 2.5 while at low numbers of waves it did not become as large as in the case of the thin shell.

It is interesting to note that at large numbers of waves ($n = 22$ for $h = .0032$ and $n = 13$ for $h = .020$) that the ratio of damping factors:

$$\frac{\tau_{.0032}}{\tau_{.020}} \approx \frac{1}{2}$$

and the ratio of frequencies:

$$\frac{f_{.0032}}{f_{.020}} \approx \frac{1}{2}$$

This resulted in $g = .0025$ approximately for both shells. This value of "g" is double the value found by Read & Graham (4) in carefully conducted experiments on electrodeposited copper. The average value they found was between .0010 and .0014.

As a further check of the damping the variation of steady state vibration amplitude with frequency near resonance was found for a number of the modes on the

h = .020 shell (see n = 9, Figure 14(a) for example). The "peak width" Δf at .707 $\delta_{o\,max}$ then yielded the damping as follows:

$$q = \frac{\Delta f}{f_{resonance}}$$

and

$$\tau = \pi f_{res} q$$

The values of τ so found are shown in the dotted curves of Figures 12 and 13 and indicate order of magnitude agreement with results of vibration decay measurements, being between 5% and 50% higher. It should be emphasized that the values determined by vibration decay are the more accurate.

At the outset it was suspected that the motions of the shell would transfer energy to the ambient air and in so doing damp the vibrations.

Calculations were made of the effects of the external air and air trapped between the shell and the support fixture by H. D. Krumhaar (5) for this configuration. Removal of the damping effects of the air from the experimental values reduced the damping coefficients by only 2 to 3%. It would appear therefore that the

aerodynamic effect was not responsible for the large increase in damping at the low values of n.

During the course of the investigation it had been suggested that the proximity of the coil of the shaker to the shell might be a source of damping due to the motion of the shell through the field of the permanent magnet. This was found to be negligibly small by obtaining almost identical results with the loudspeaker excitation.

One other type of damping often encountered is boundary damping. Lambert and Taok (6) indicate that boundary damping is of primary importance at low mode numbers but the effect of internal material damping becomes important at high mode numbers. This agrees qualitatively with the results of this study.

C. Experimental Difficulties

It should be noted that the close proximity in frequency of the modes of the thinnest shell made analysis of the modal patterns very difficult even though the resonances seemed adequately separated to permit accurate frequency measurement. The superposition of waves of nearby modes often resulted in complicated amplitude

patterns when plotted circumferentially. Careful positioning of the sensor axially and to a certain extent selective positioning of the exciter usually caused the mode under investigation to stand out sufficiently to be recognized. It is doubtful, however, that shells of smaller thickness can be analysed in this manner.

On the other hand, all modes investigated on the h = .020 inch shell gave quite regular modal patterns even in the single case of mode interference.

Another effect of mode interference is illustrated in Figure 14. It appears to be a beating between the mode under investigation and its neighbor, or an oscillating exchange of energy. The beating does not occur during steady state forced oscillation but seems to come into play during the subsidence as shown for the attempted decay measurements of modes $n = 7$ and $n = 8$ on the $h = .020$ shell. The steady state interference is shown as a function of frequency in Figure 14(a). It should be noted that modes for which no τ is shown in Figures 10 to 13 were those for which this type of interference was too large to allow the damping to be determined.

IV. CONCLUSIONS

The fundamental frequencies agreed to within 10% of the theoretical values for fixed ends and the modes agreed to within one circumferential wave. For modes of higher numbers of waves the agreement was even closer. For modes of lower numbers of waves where end fixity was important the experimental values fell between the theoretical curves for fixed and freely supported ends.

The damping factors τ , of a given shell, were fairly constant for modes with greater numbers of waves than the fundamental. For modes with numbers of waves less than the fundamental, however, the damping increased rapidly as the numbers of waves reduced; with the thinner shell exhibiting the greater rise.

At the highest wave number tested on each cylinder the effective structural damping parameter $g \approx .0025$. This value was approximately double that found for electrodeposited copper by Read and Graham.

The contribution of ambient and internal air to the damping was small for the frequencies tested.

Boundary damping may be an important contributor to the total damping.

REFERENCES

1. Arnold, R. N., and Warburton, G. B., The Flexural Vibrations of Thin Cylinders, Journal and Proceedings of the Institution of Mechanical Engineers (London), Vol. 167, pp. 62-74, 1953.

2. Reissner, E., On Transverse Vibrations of Thin Shallow Elastic Shells, Quarterly of Appl. Math., Vol. 13, No. 2, pp. 169-176, July, 1955.

3. Rife, D. O., and Edgell, A. D., Induction Vibration Equipment Development, Engineering Research Report-PO-026, Dynamics, Convair/Pomona, Nov. 4, 1960.

4. Read, Harold J., and Graham, Arthur H., The Elastic Modulus and Internal Friction of Electrodeposited Copper, Journal of the Electrochemical Society, Vol. 108, No. 1, pp. 73-78, January, 1961.

5. Krumhaar, H. D. (Report to be published)

6. Lambert, R. F., and Tack, D. H., Influence of Natural Frequencies and Source Correlation Fields on Random Response of Panels, Wadd Technical Report 60-188, July, 1960.

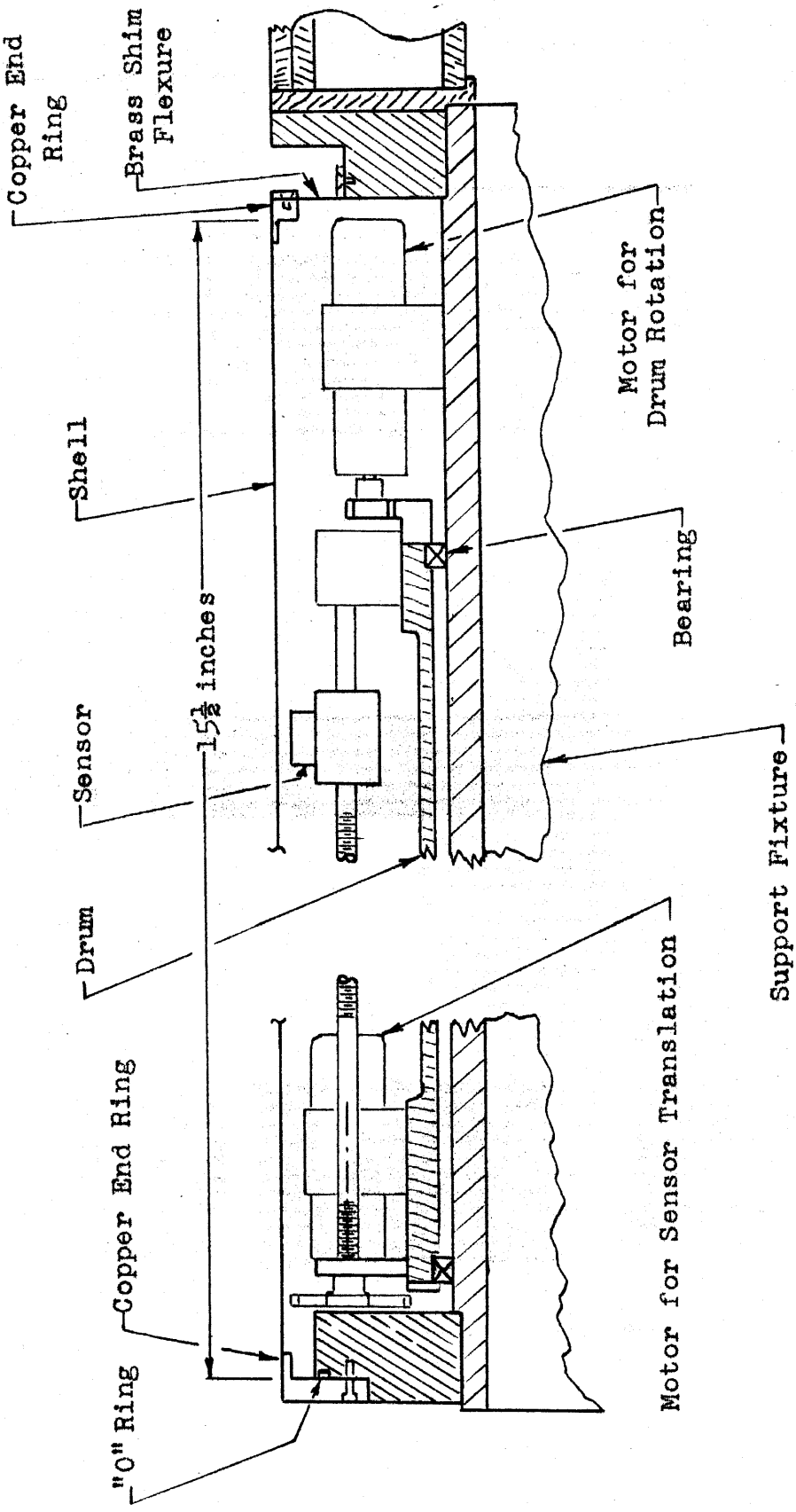

Fig. 1 Vibration Sensor and Shell Assembly

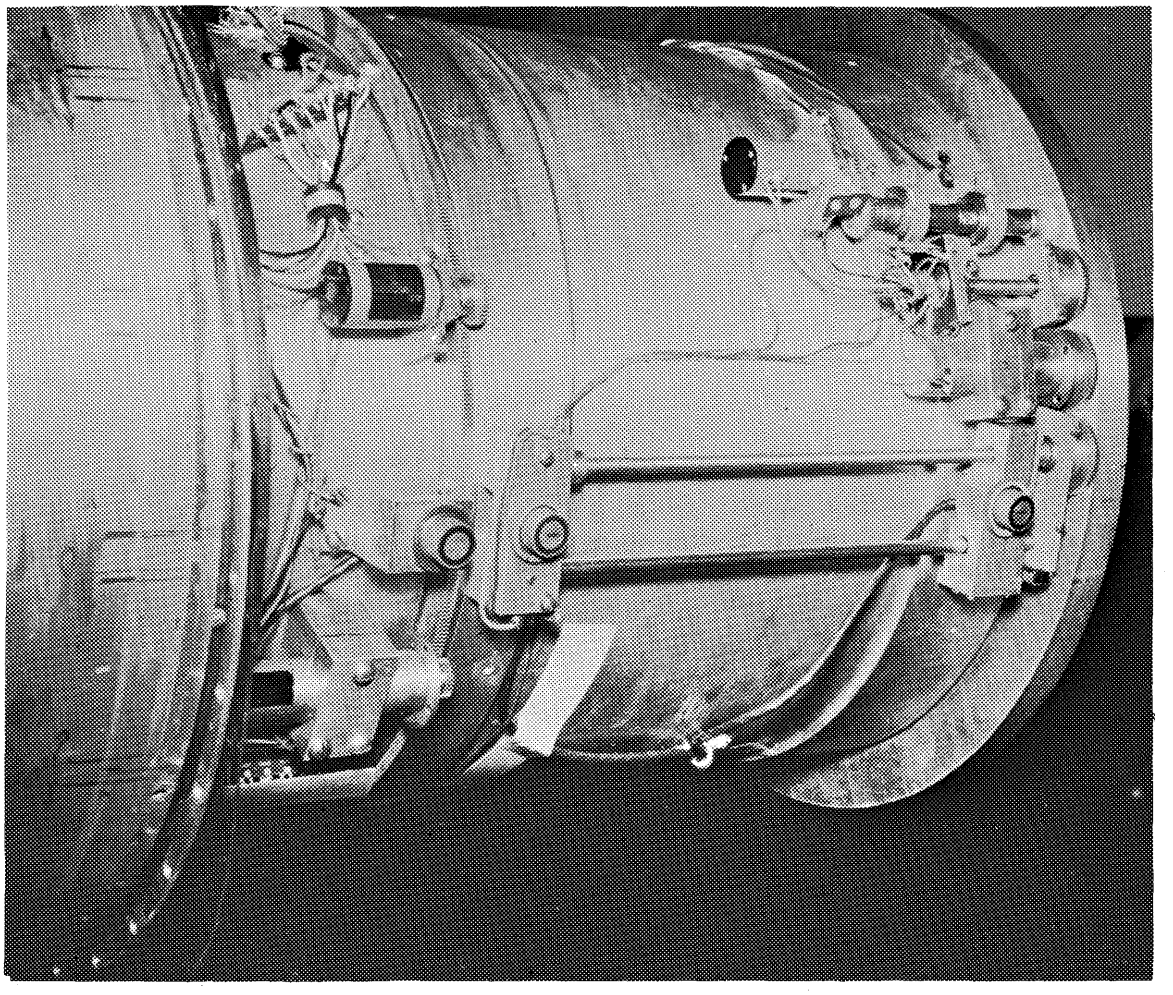

Fig. 2 General Arrangement of Sensors, Traversing Mechanism and Position Indicators.

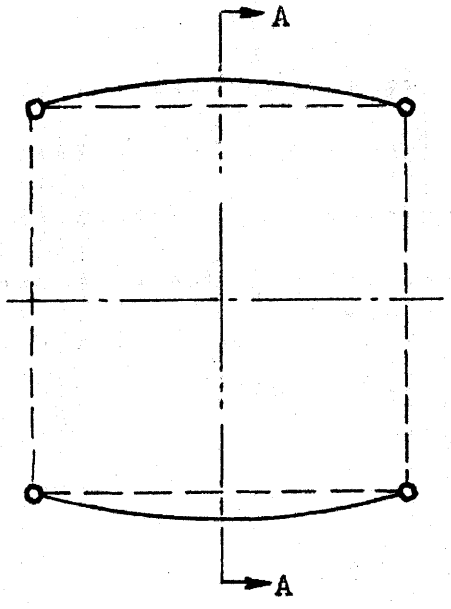

Ends Freely Supported
m = 1

Section A-A

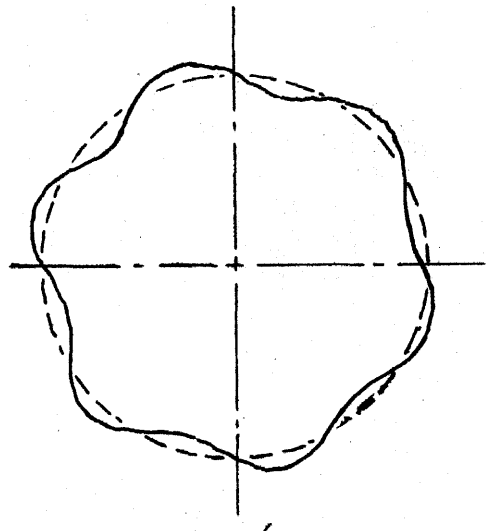

n = 6

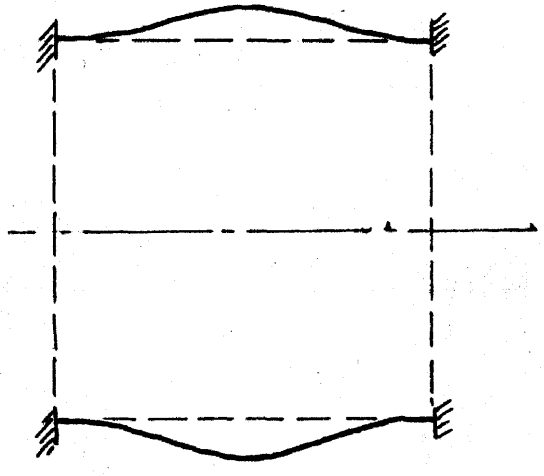

Ends Fixed
m = 1

Note: The terms "fixed" or "freely supported" imply, in this report, no restraint in the axial or circumferential direction at the boundaries.

Fig. 3 Modal Geometry

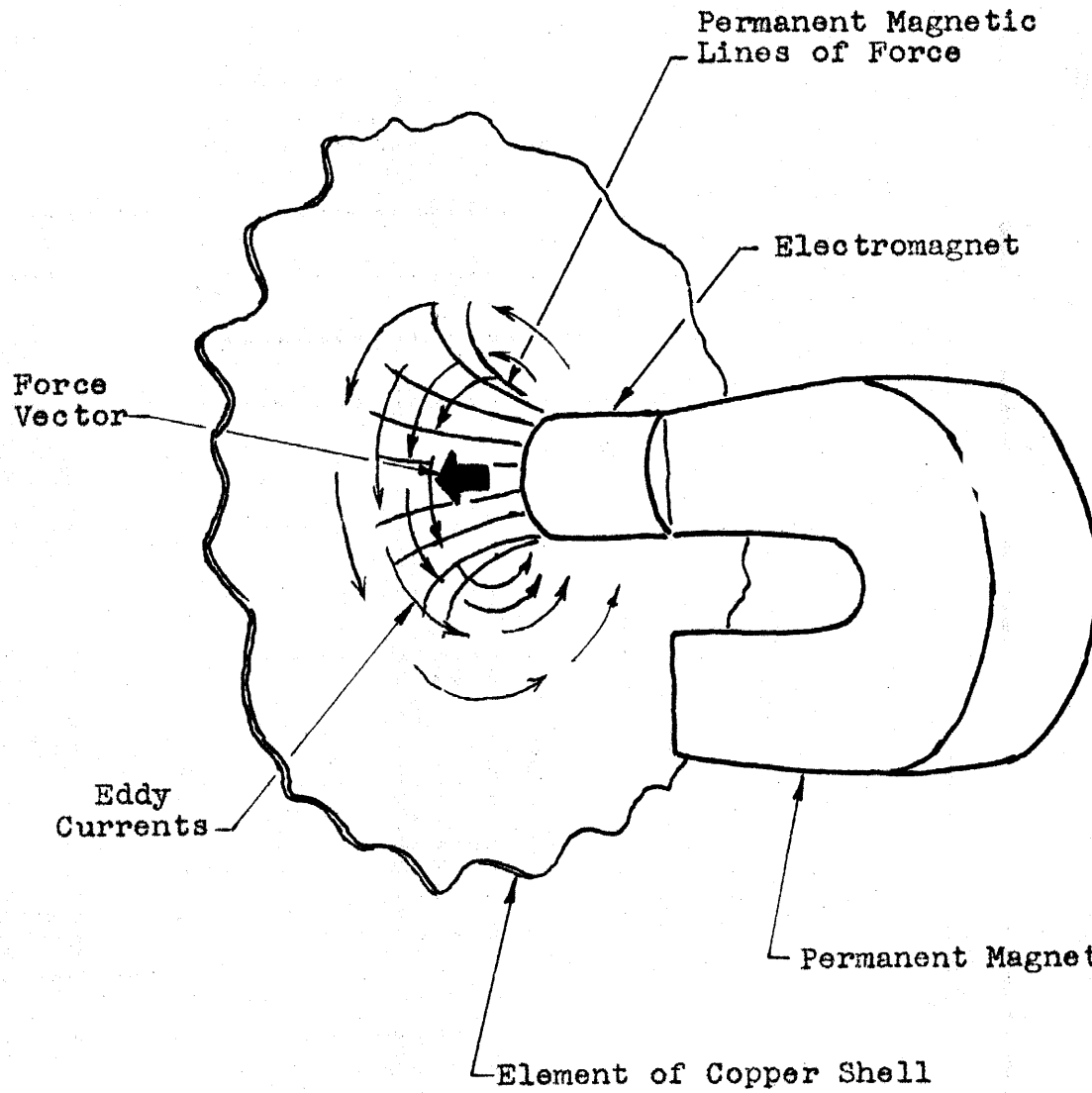

Fig. 4 Geometry of the Forces, Fields and Currents for the Electrodynamic Shaker.

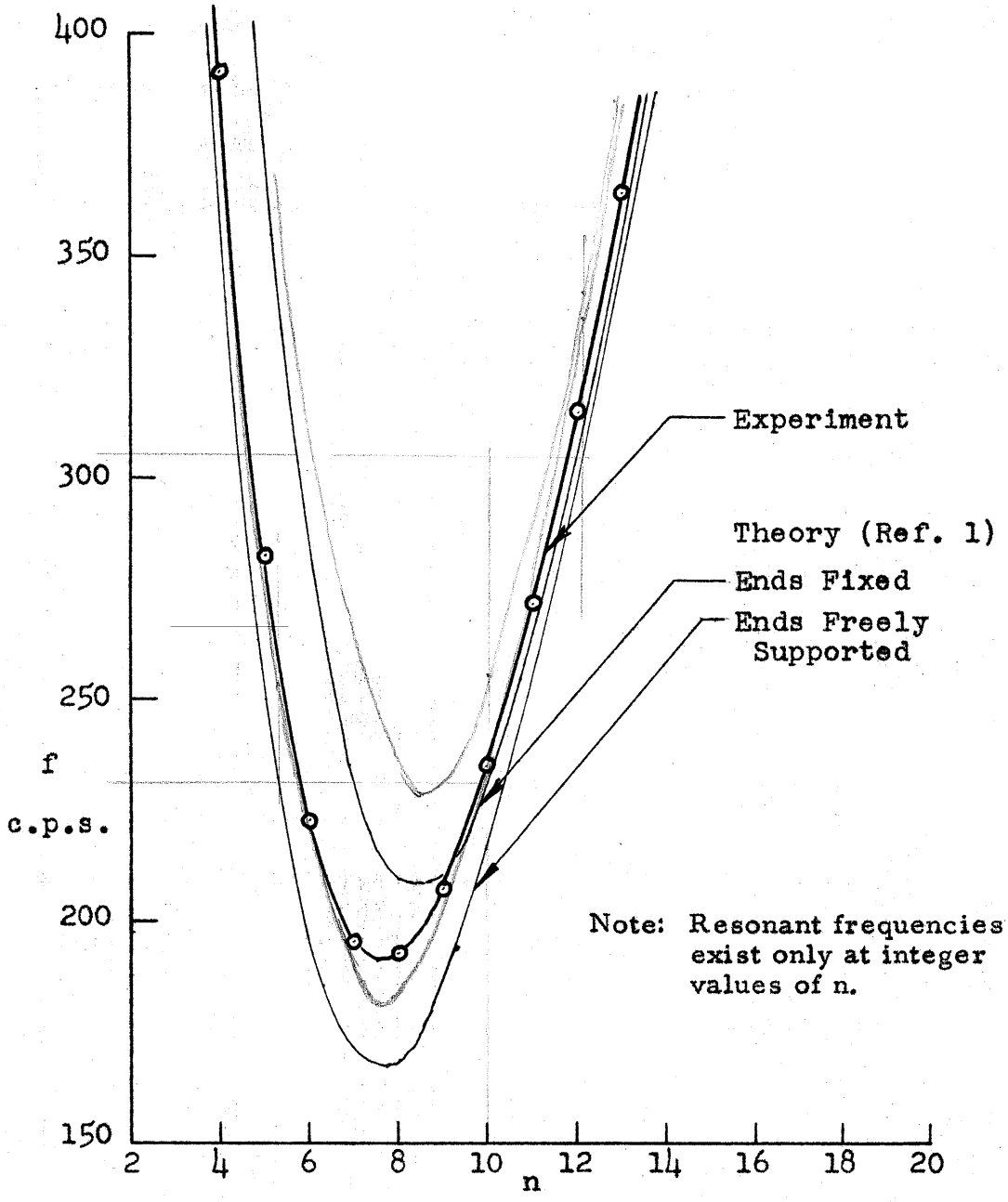

Fig. 5 Resonant Frequency vs. No. of Circumferential Waves for h = .020 inches; m = 1.

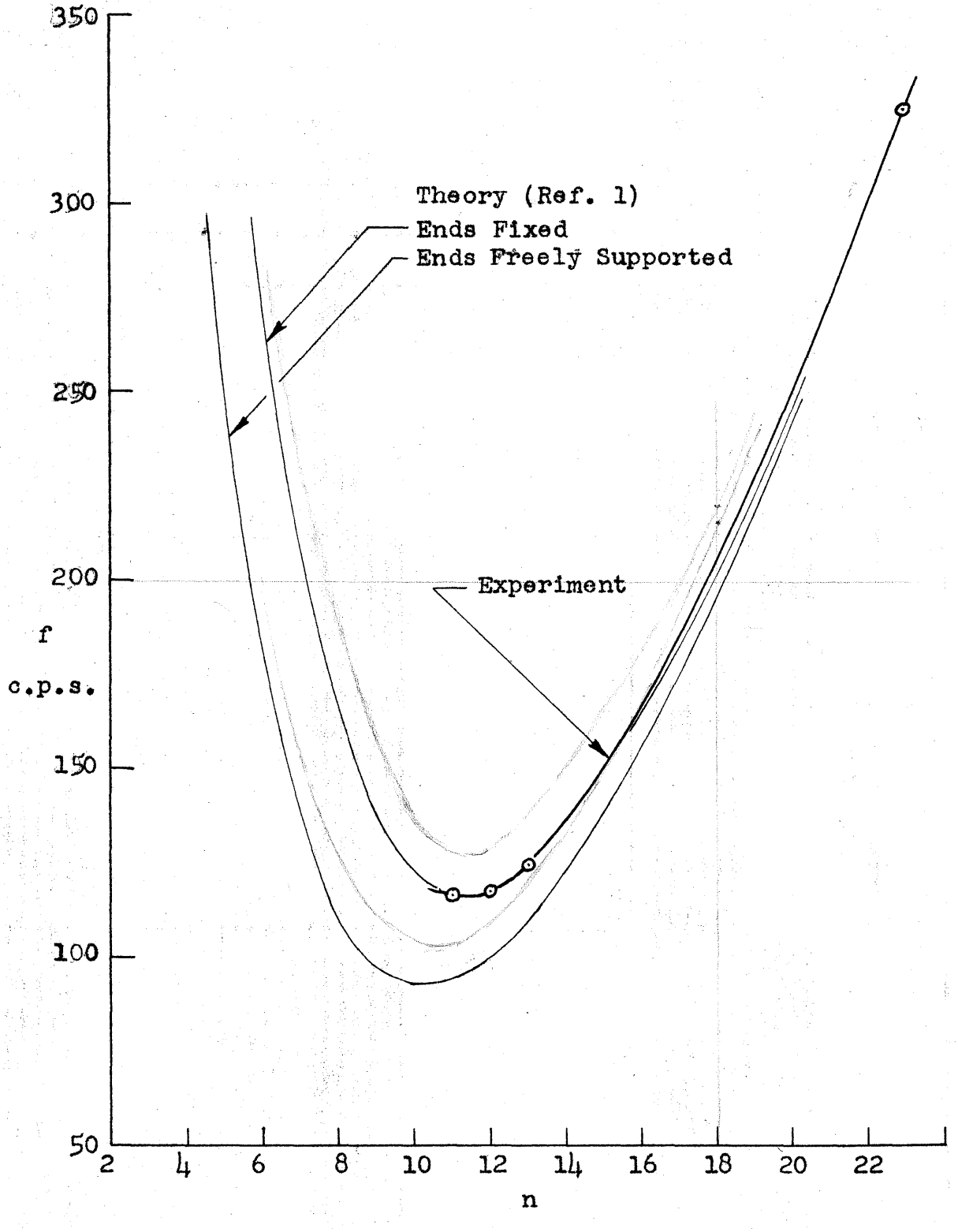

Fig. 6 Natural Frequency vs. No. of Circumferential Waves for m = 1; h = .0060 inches.

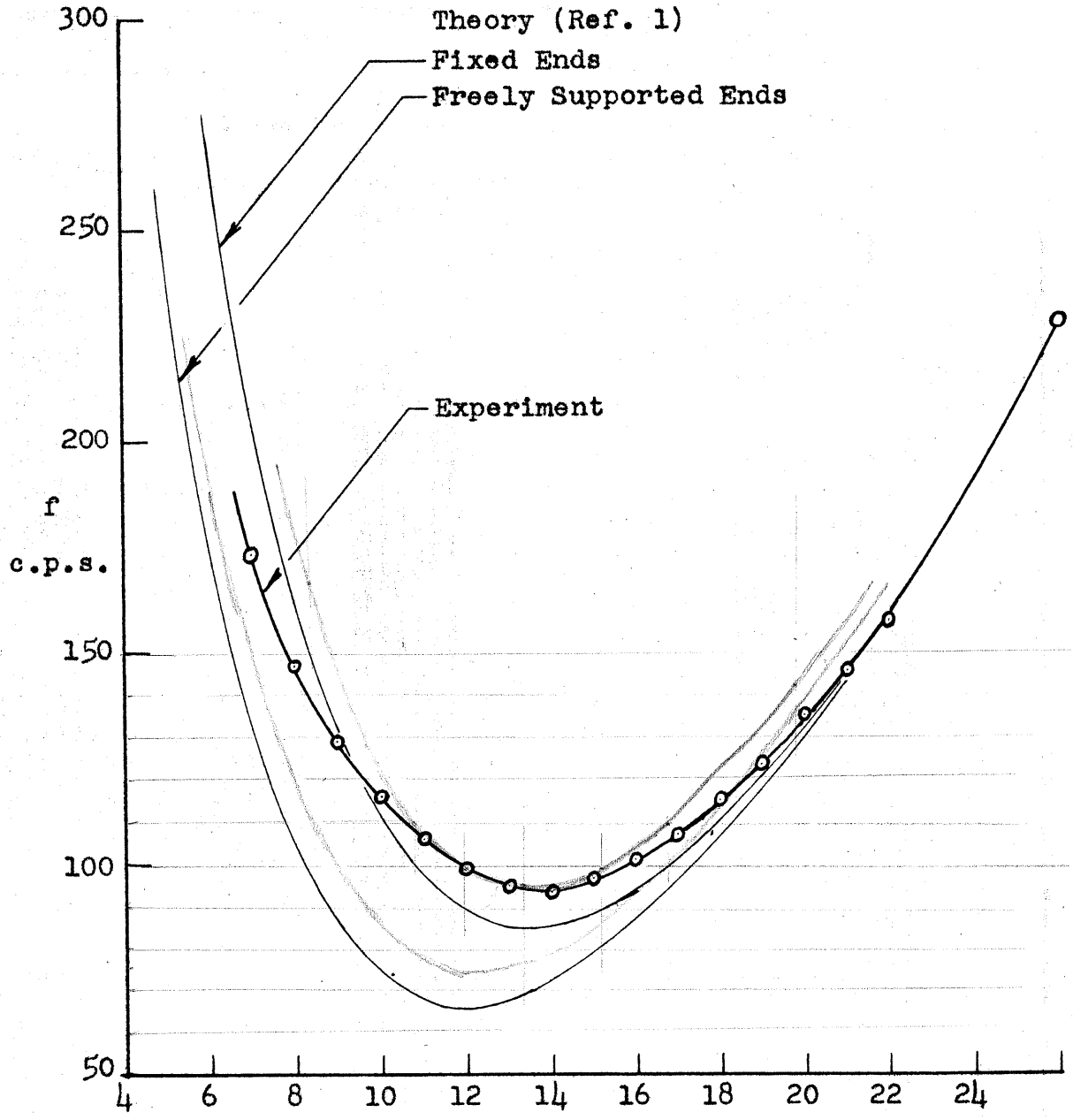

Fig. 7 Natural Frequency vs. No. of Circumferential Waves for m = 1; h = .0032 inches.

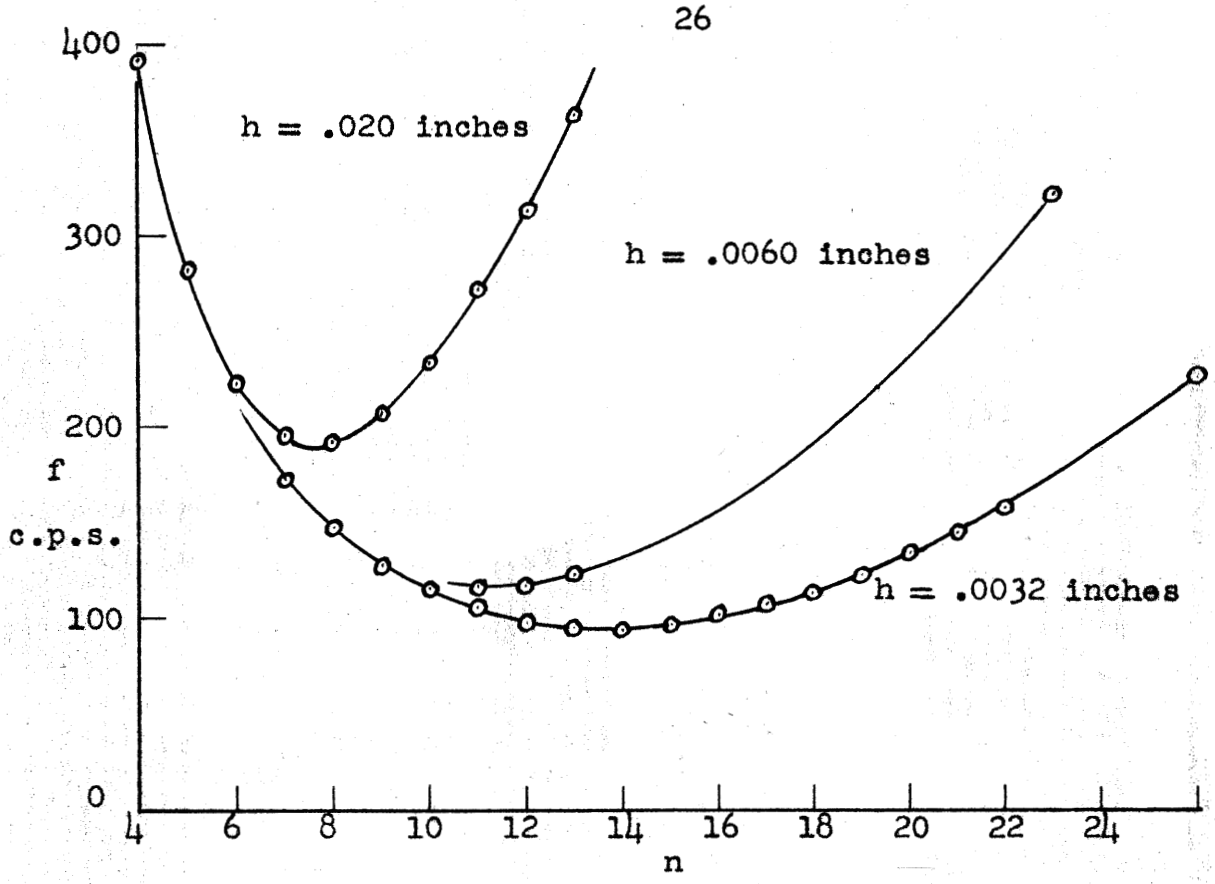

Fig. 8 Effect of Wall Thickness on Natural Frequency (Experimental)

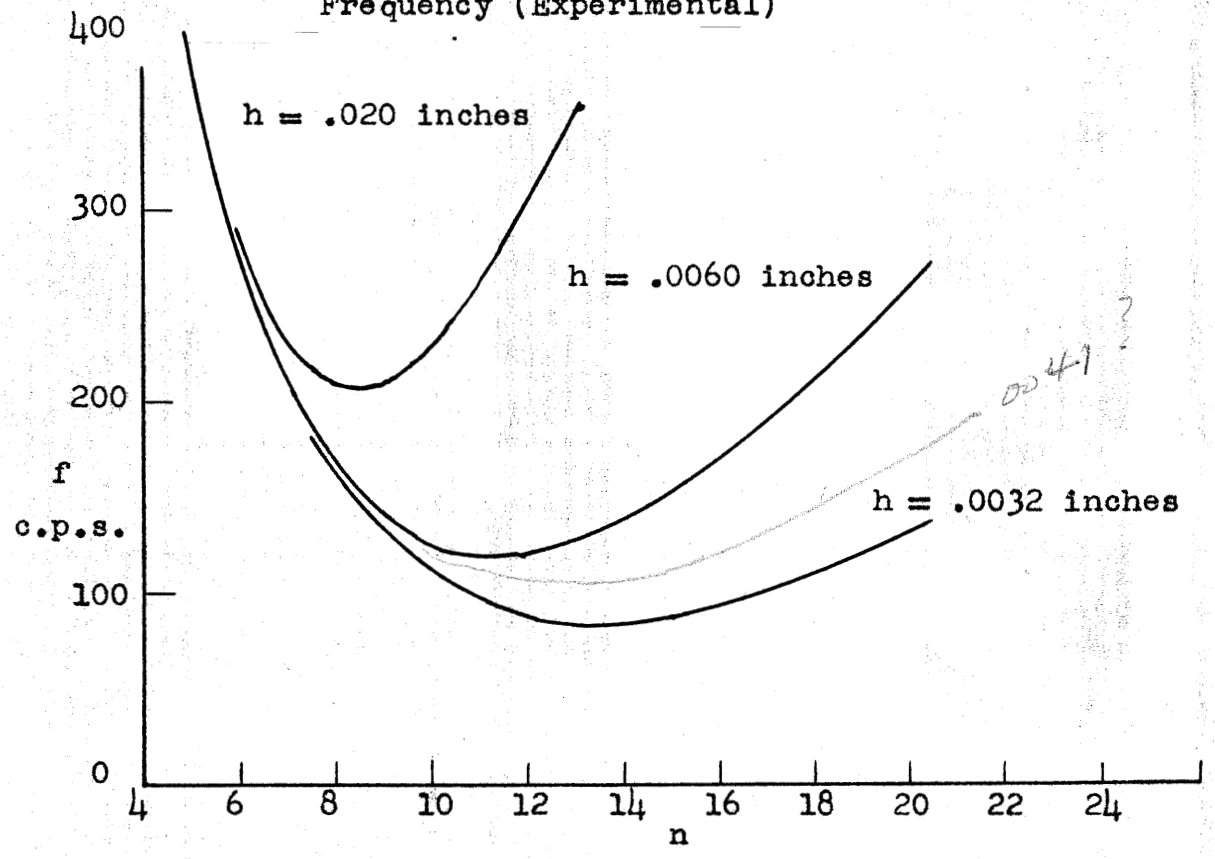

Fig. 9 Effect of Wall Thickness on Natural Frequency (Theoretical, Fixed Ends)

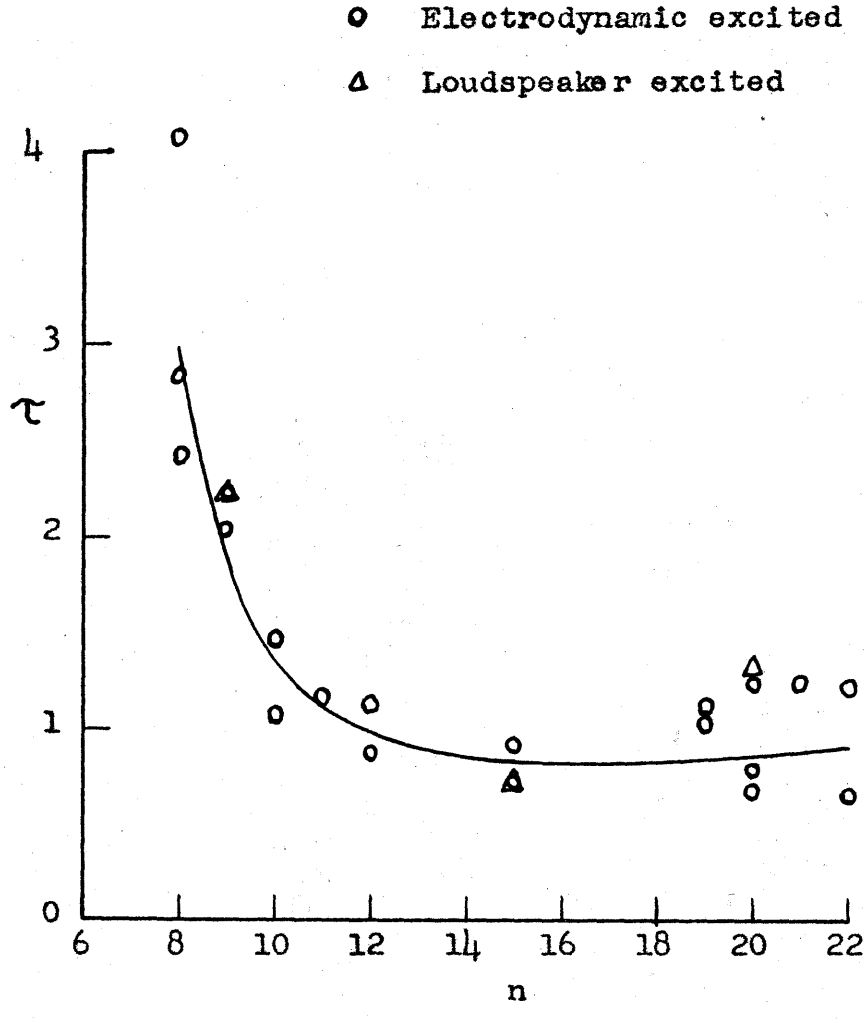

Fig. 10 Damping Factor vs. Circumferential Waves for h = .0032 inches; m = 1.

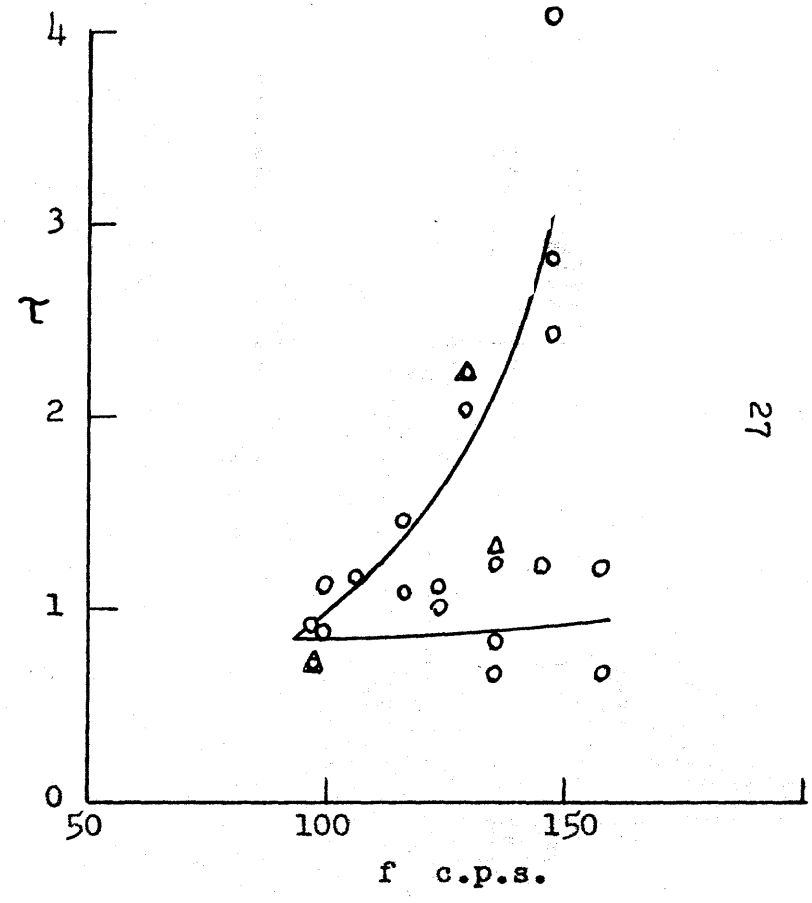

Fig. 11 Damping Factor vs. Natural Frequency for h = .0032 inches; m = 1.

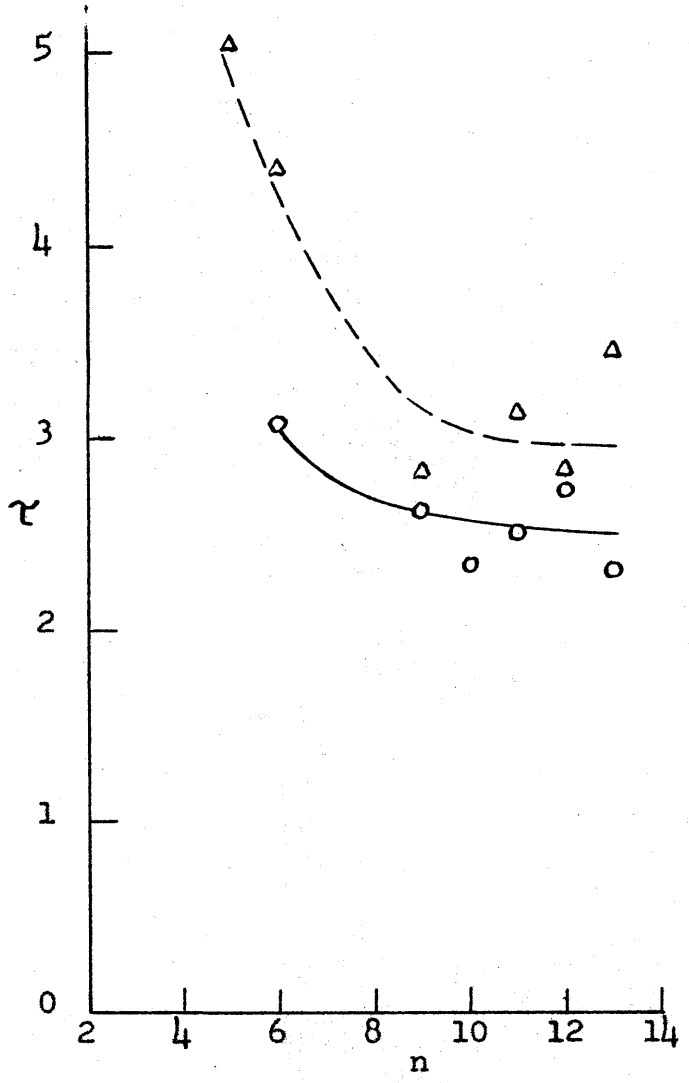

Fig. 12 Damping Factor vs. Circumferential Waves for h = .020 inches; m = 1.

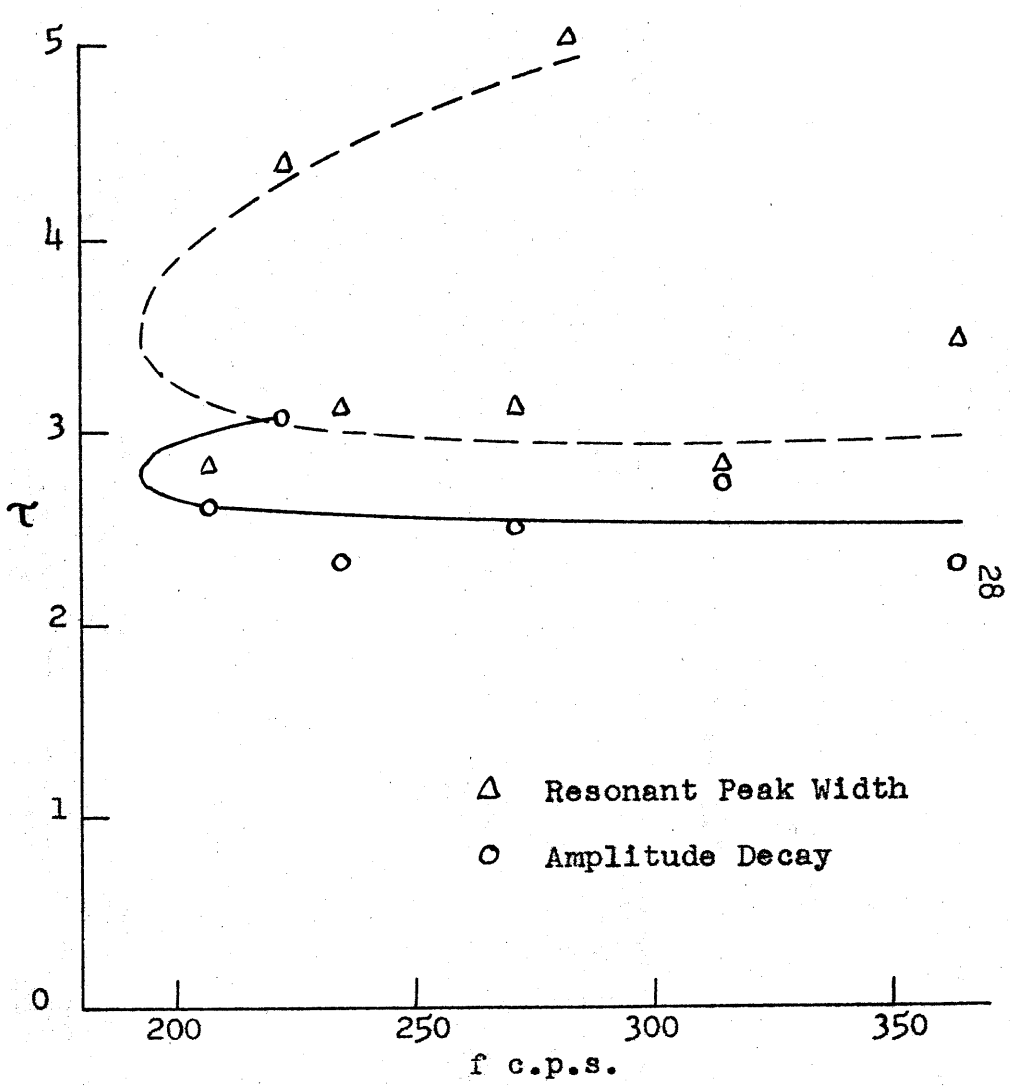

Fig. 13 Damping Factor vs. Natural Frequency for h = .020 inches; m = 1.

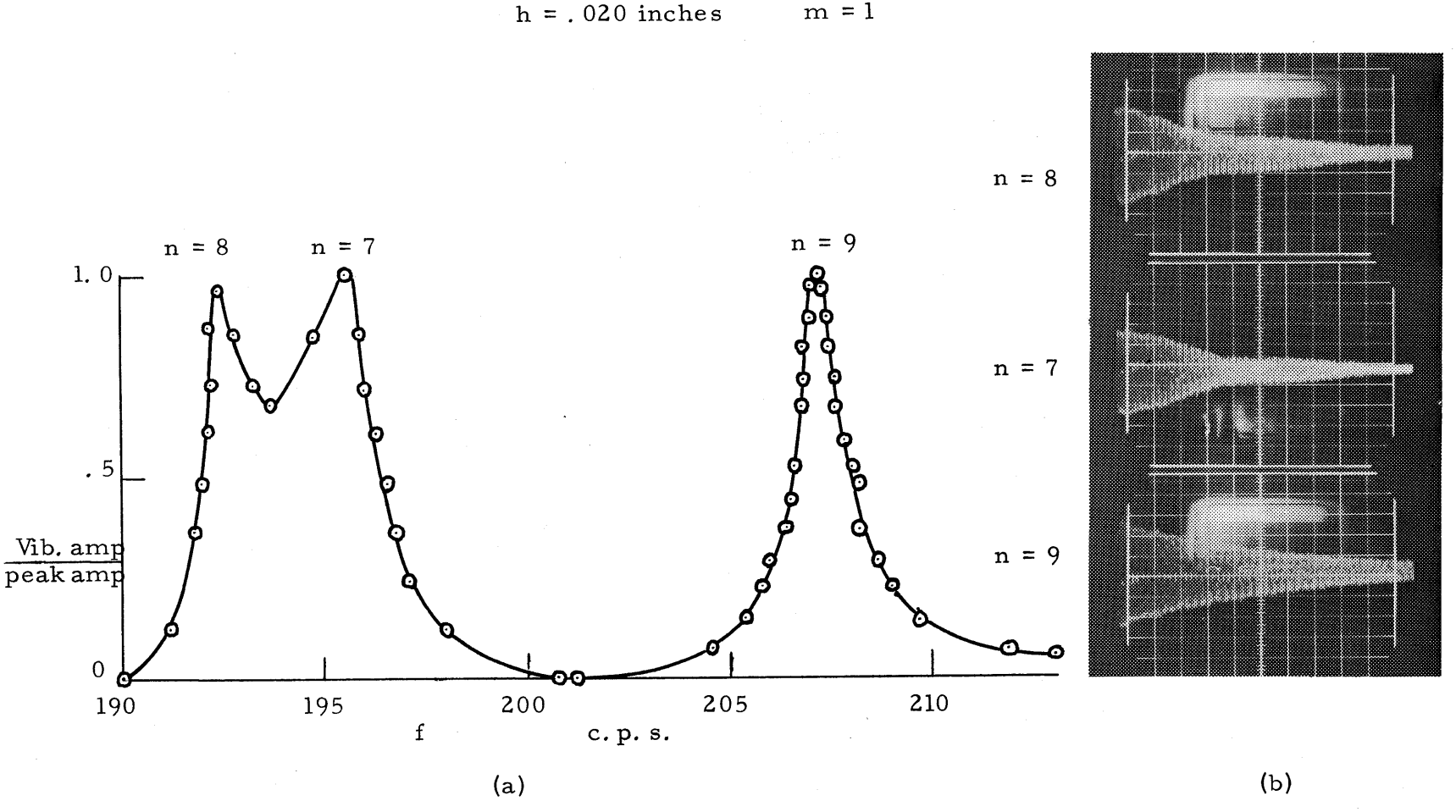

Fig. 14 Effect of Small Frequency Difference Between Two Modes on (a) Resonant Response (b) Time Decay; and Comparison With an Isolated Mode.

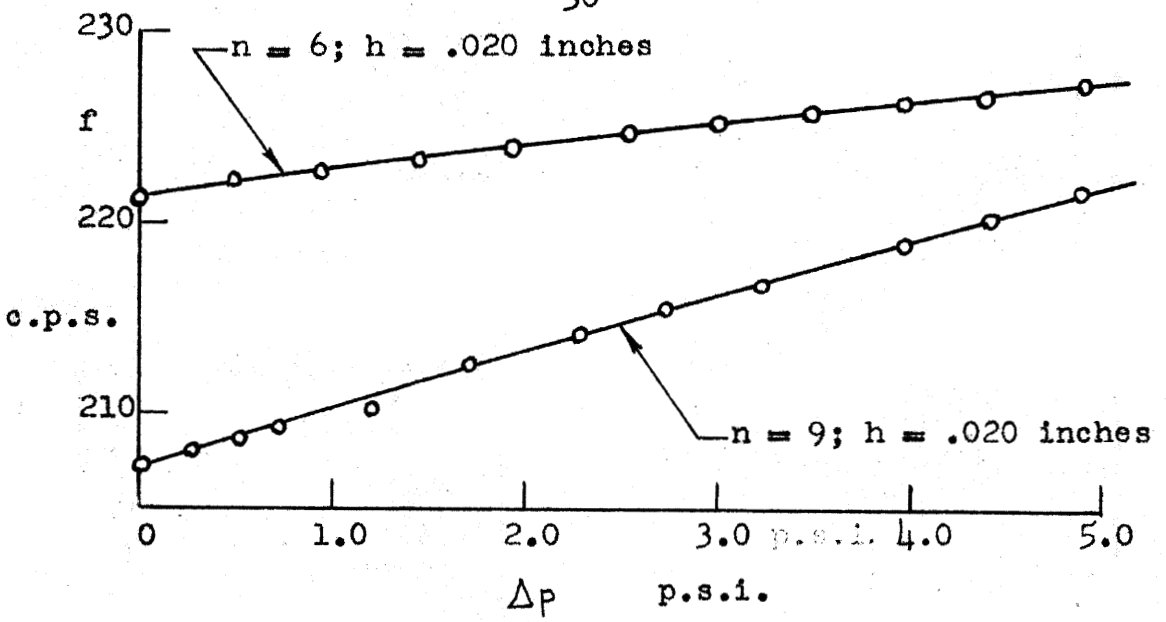

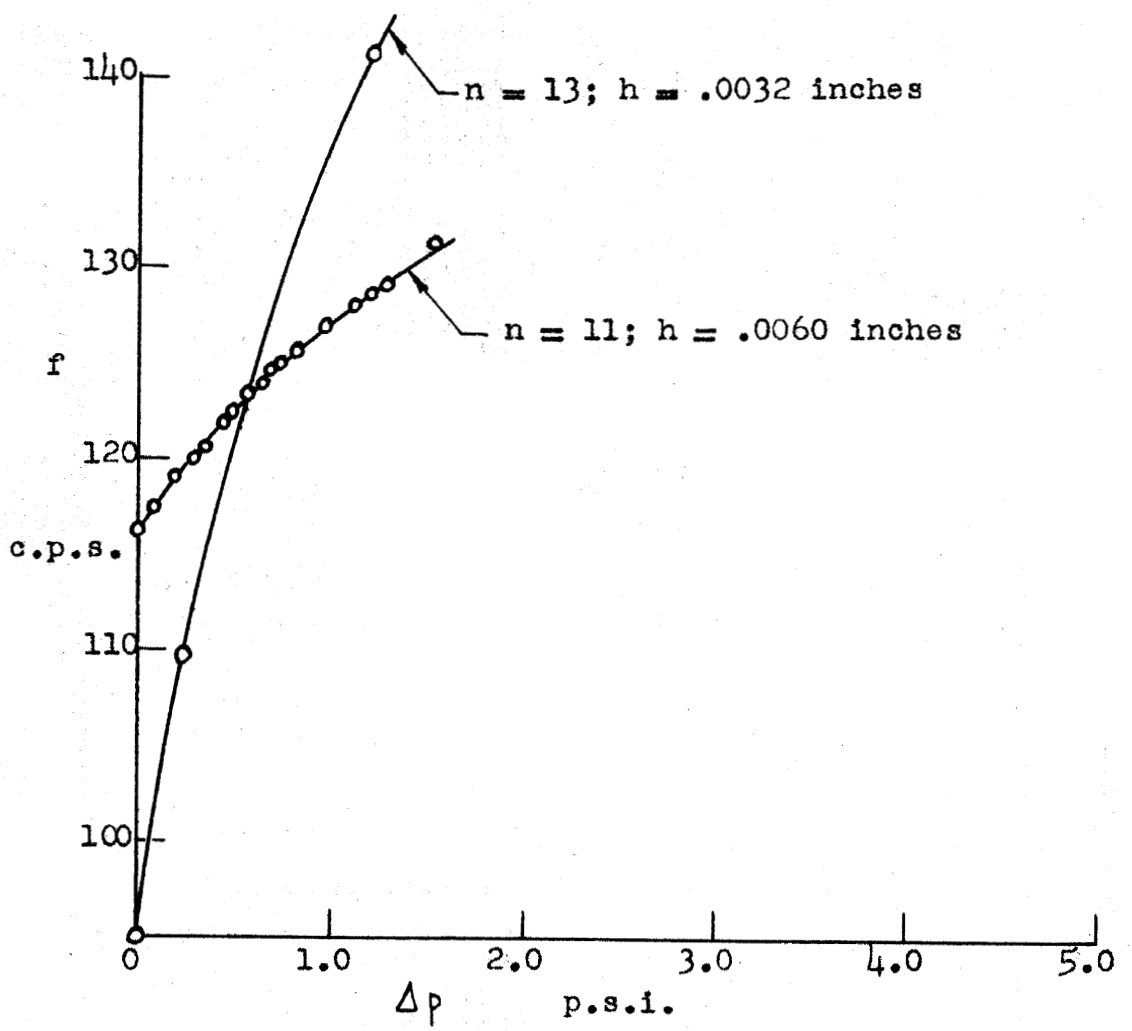

Fig. 15 Effect of Internal Pressure on Resonant Frequency; m = 1.